Visible Emission Tomography in the H-1NF Heliac

Fenton Glass, John Howard, and Boyd Blackwell

***Abstract*—A tomographic visible Doppler spectroscopy system has been used to generate images of ion spectral-line brightness for low-field radio-frequency (RF) heated argon discharges in the H-1NF heliac. Unconstrained tomographic reconstructions for a number of different plasma regimes are presented.**

***Index Terms*—Computer tomography, Doppler spectroscopy, magnetic surfaces.**

PROJECTIONS of Doppler-broadened argon ion emission (488 nm) in low-field radio-frequency (RF) heated discharges in the H-1NF heliac have been obtained using an array of lens-coupled optical fibers that encircle the plasma poloidal cross section. The collected light is transmitted to a coherence imaging camera [1] which processes the spectral information to produce line-integrated estimates of the brightness, brightness-weighted temperature, and brightness-weighted plasma flow speed. In this paper, we present images of relative ion spectral-line emission intensity for a number of different confinement regimes that have been tomographically inverted without recourse to imposed assumptions or constraints. To our knowledge, these are the first reported tomographic reconstructions of visible ion emission produced without *a priori* restrictions.

The light-collection system consists of five identical modules each housing 11 parallel lens-coupled optical fibers. The modules are mounted at intervals of 45° on the rim of a rotatable carrier ring which poloidally encircles the plasma. The carrier ring is supported by a C-frame with both residing in the vacuum tank. During rotation, the optical fibers are spooled onto the ring circumference, allowing the viewing modules to be moved by up to 200°. For sufficiently reproducible plasmas, the ring can be rotated, on a shot-to-shot basis, to a number of distinct viewing stations to improve the sampling of the sinogram. Details of the optical system are reported elsewhere [2]. Fig. 1 is a photograph of the light-collection system installed between the toroidal field coils.

Large core (1 mm) silica fibers transmit the light to the coherence-imaging spectrometer, which is external to the vacuum tank. This spectrometer is a field-widened imaging polarization interferometer that utilizes an electrooptic, birefringent crystal modulated about a fixed delay to characterize the coherence of a spectrally isolated emission line. The interference fringes

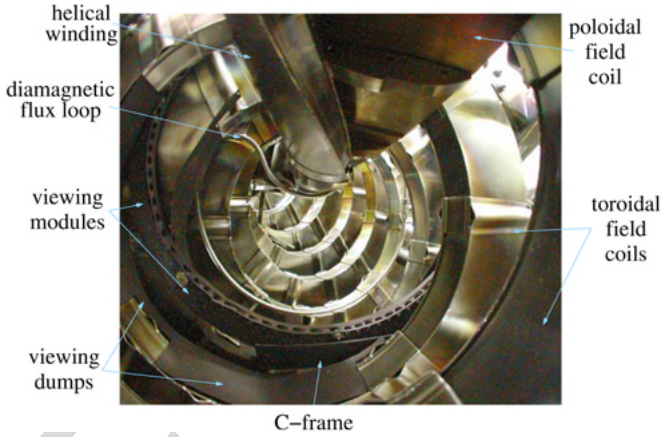

Fig. 1. Photograph showing the in-vacuum light-collection system, consisting of five viewing modules, with 11 lens-coupled optical fibers each, mounted on a rotatable carrier ring, encircling the plasma region.

are imaged onto an 8×8 multianode photomultiplier array, allowing time-resolved measurements of the low-order moments of the ion velocity distribution function using a single detector per line-of-sight channel. The results presented in this paper are restricted to the measured brightness, with measurements of the ion temperature and bulk flow velocity to be reported elsewhere.

The entire system requires a careful calibration procedure to determine, for each channel, the spatial response in the plasma region, the interferometer instrument function, the relative channel sensitivity, and the effects of crosstalk in the detector and optical system. These quantities are determined utilizing miniature fluorescent tubes mounted inside the vacuum within the field of view of the rotating ring, and, for the interferometer, a monochromatic light source at or near the wavelength of the selected spectral line.

The H-1NF heliac has three field periods and can access a wide range of magnetic configurations [3]. By altering the ratio of the currents in the various control coils and the main toroidal field coil set, the rotational transform can be varied between $\sim$1.0–2.0 and the poloidal cross-sectional shape can be changed significantly. Fig. 2(a) and (b) shows the reconstructed brightness for the "standard" magnetic field configuration (no current in the helical control winding, on-axis transform $\approx$1.1) for on-axis field strengths of 0.043 and 0.16 T, respectively. Fig. 2(c) shows brightness contours for a bifurcated field configuration having rotational transform near 0.5 per field period and field strength of 0.11 T. This atypical configuration was deliberately chosen to test the system imaging capability.

Poincaré plots of the computed magnetic flux surfaces at the position of the light-collection system are shown superimposed over the brightness reconstructions. For all reconstructions, data obtained at different viewing stations for nominally identical discharges are normalized in brightness using signals from a

Manuscript received August 12, 2004.

F. Glass and B. Blackwell are with the Plasma Research Laboratory, Australian National University, Canberra ACT 0200, Australia (e-mail: fenton.glass@anu.edu.au).

J. Howard is with the Plasma Research Laboratory, Australian National University, Canberra ACT 0200, Australia and he is also with the Department of Electrical and Computer Engineering, Texas Tech University, Lubbock, TX 79409 USA (e-mail: john.howard@anu.edu.au).

Digital Object Identifier 10.1109/TPS.2005.845900

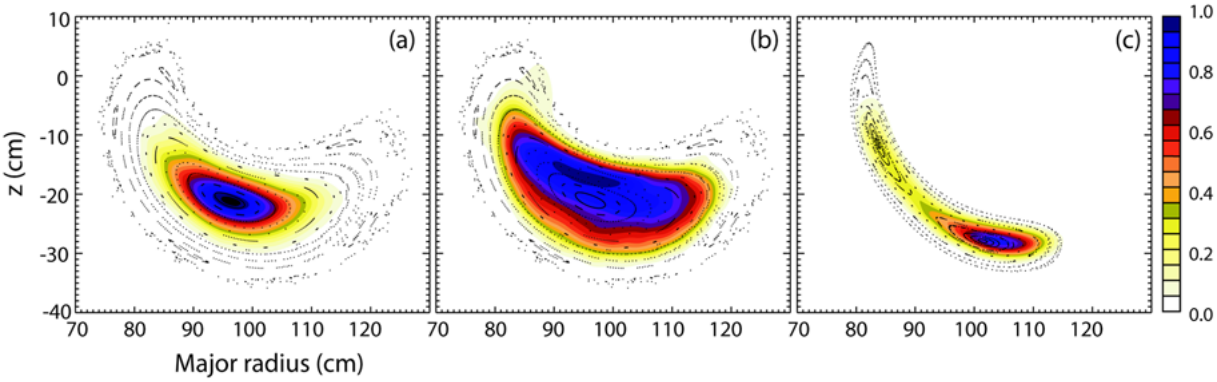

Fig. 2. Tomographic reconstructions of argon ion spectral-line brightness for (a) low field (0.043 T) standard magnetic configuration, (b) higher field (0.16 T) standard magnetic configuration, and (c) birfurcated configuration near rotational transform of 0.5 per field period. Poincaré plots of the calculated magnetic flux surfaces at the toroidal position of the light collection system are shown superimposed on the reconstructions.

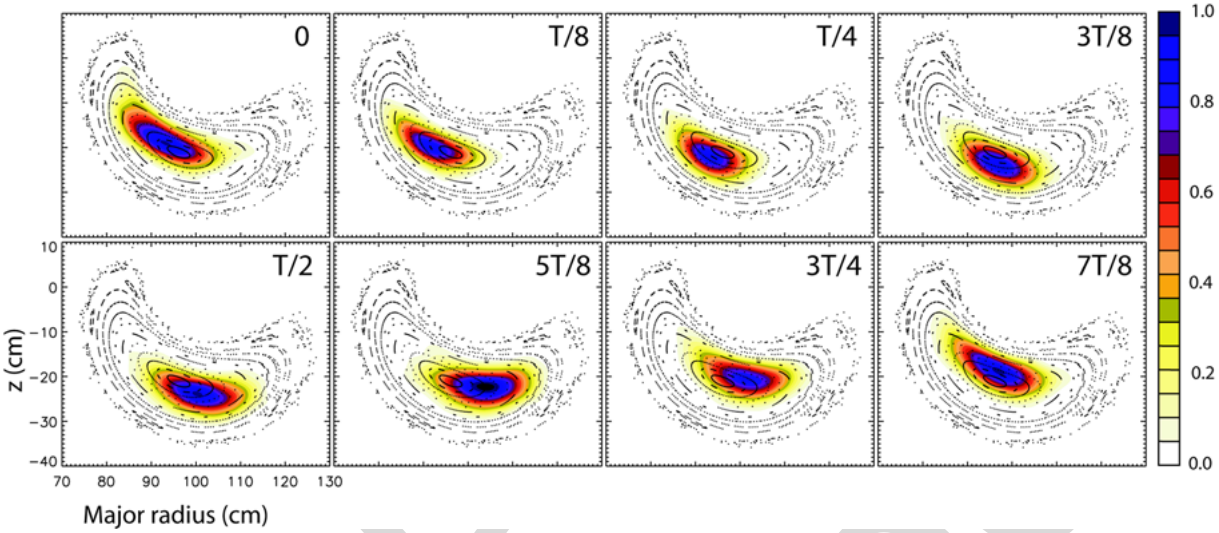

Fig. 3. Reconstruction of argon ion spectral-line brightness at equispaced phases during an unstable low-field (0.043 T) plasma discharge in standard magnetic configuration.

fixed-view coherence-imaging camera. Given the relatively dense sampling of the sinogram, a total of 344 line-integrated measurements for Fig. 2(a) and (b) and 500 for Fig. 2(c), an iterative arithmetic reconstruction technique (ART) [4] was sufficient to obtain consistent and reliable reconstructions.

The low-field standard configuration reconstruction [Fig. 2(a)] conforms closely with the computed flux surfaces. At higher fields [Fig. 2(b)], there is a significant shift in the emission peak and a broadening of the profile. The asymmetry, which is also observed by the fixed-view camera, may be related to a change in the nature of the coupling between the helicon-mode RF heating antenna and the plasma.

Under certain discharge conditions in standard configuration, a global coherent instability can be observed (fill pressure $\sim 3 \times 10^{-5}$ torr, RF heating power 60 kW, on-axis magnetic field strengths 0.043–0.13 T). This mode is sufficiently reproducible to allow consistent measurements to be obtained at a number of independent observing stations. To improve the signal-to-noise ratio, light signals are averaged over many oscillation periods with Mirnov coil signals used to synchronize independent data sets and to track small drifts in mode frequency. Fig. 3 shows the brightness reconstructions at equispaced phases of the mode rotation (period $\mathrm{T} \approx 0.32$ ms). Note that Fig. 2(a) shows the direct current (dc) component of the brightness associated with this mode. The large oscillating shift in the brightness center-of-mass has also been observed in the density using the scanning tomographic interferometer.

Acknowledgment

The authors wish to thank C. Michael for signal processing assistance.

References

[1] J. Howard, C. Michael, F. Glass, and A. Danielsson, "Time-resolved two-dimensional plasma spectroscopy using coherence-imaging techniques," *Plasma Phys. Control. Fusion*, vol. 45, pp. 1143–1166, Jul. 2003.

[2] J. Howard, C. Michael, F. Glass, and A. D. Cheetham, "Optical coherence techniques for plasma spectroscopy," *Rev. Sci. Instrum.*, vol. 72, pp. 888–897, 2001.

[3] S. M. Hamberger, B. D. Blackwell, L. E. Sharp, and D. B. Shenton, "H-1 design and construction," *Fusion Technol.*, vol. 17, pp. 123–130, Jan. 1990.

[4] S. R. Deans, *The Radon Transform and Some of Its Applications*. Melbourne, FL: Krieger, 1993.